Available online at www.sciencedirect.com
ScienceDirect
Thermochimica Acta 455 (2007) 129–133
thermochimica acta
www.elsevier.com/locate/tca

# Oxidation behavior of the simulated fuel with dissolved fission products in air at 573–873 K

K.H. Kang [a,*], S.H. Na [a], K.C. Song [a], S.H. Lee [b], S.W. Kim [c]

[a] *Korea Atomic Energy Research Institute, P.O. Box 105, Yuseong, Daejeon 305-600, Republic of Korea*
[b] *Korea Research Institute of Standards and Science, P.O. Box 102, Yuseong, Daejeon 305-600, Republic of Korea*
[c] *Department of Physics, University of Ulsan, Ulsan 680-749, Republic of Korea*

Available online 30 November 2006

**Abstract**

As a part of the DUPIC fuel development program, oxidation behavior of the simulated spent fuel with dissolved fission products has been studied using a thermogravimetry analyzer in the temperature range of 573–873 K in air in order to establish the oxidation temperature and time of the OREOX process during fabrication of DUPIC fuel. Oxidation behavior of an $UO_2$ sintered pellet has also been measured for the purpose of comparison. From the XRD study, the simulated spent fuel has been converted to $U_3O_8$, in the temperature range of 573–873 K. The oxidation curves of the simulated spent fuel are displayed sigmoidal reaction kinetics which follows the nucleation-and growth mechanism of the formation of $U_3O_8$. The fission products forming the solid solution in $UO_2$ matrix delayed $U_3O_8$ forming. Activation energies of the simulated spent fuel are higher than those of $UO_2$. There are transition points in the rate of the oxidation of the simulated fuel and $UO_2$ between 673 and 723 K, and the activation energies in the low temperature range of 573–673 K are higher than those in the high temperature range of 723–873 K.


*Keywords:* Oxidation; DUPIC fuel; Simulated spent fuel; Solid solution; Activation energy

## 1. Introduction

Information on oxidation behavior of oxide nuclear fuel is necessary for evaluation of its stability during irradiation in a reactor because the O/U (oxygen/uranium) ratio affects the thermal properties such as the melting point, specific heat, thermal expansion and thermal conductivity. It is also required to establish the OREOX (oxidation and reduction of oxide fuel) process during fabrication of DUPIC (direct use of fuel spent PWR fuel in CANDU reactor) fuel [1,2] and to evaluate its stability for a long-term storage and disposal of spent fuel. The importance of the oxidation behavior of nuclear fuel has led to numerous experimental studies using a thermogravimetric analyzer (TGA) and an X-ray diffraction (XRD) analysis. There are extensive literatures dealing with the evaluation of oxidation behavior of nuclear fuel during the dry storage and the ultimate disposal of spent nuclear fuel [3–6]. Some papers on the effects of a deviation from a stoichiometry on the thermophysical properties of the nuclear fuel were reported [7–10].

McEachern and Taylor [11] reviewed extensive literature on the air oxidation of $UO_2$ at temperature below 673 K. They examined systematically the key parameters that affected the rate of the $UO_2$ oxidation and evaluated their importance to the reaction rate.

Griffiths and Volkovich [12] reviewed the high temperature oxidation of uranium oxides in molten salts and in the solid state to form alkali metal uranates, and their composition and properties.

For the last decade, low decontamination processes of spent fuel such as AIROX (atomics international reduction and oxidation) [13] or OREOX [2] have been considered to be promising for the reuse of spent nuclear fuel from the aspect of nonproliferation. In these processes, irradiated pellets are oxidized at around 673 K to declad and to produce sinterable powder. Both the temperature and time of the oxidation play an important role in determining the characteristics of the resultant powder. Bae et al. [14] studied the oxidation of unirradiated $UO_2$ pellets to clarify oxidation behavior, to characterize the oxidized powder and to establish a new spallation model at 673 K, as a part of the DUPIC fuel development program. However the oxidation behavior of the spent fuel is expected to be different from unirradiated $UO_2$ because there are many fission products as impurities

* Corresponding author. Tel.: +82 42 868 2565; fax: +82 42 868 2403.
*E-mail address:* nghkang@kaeri.re.kr (K.H. Kang).

0040-6031/$ – see front matter © 2006 Elsevier B.V. All rights reserved.
doi:10.1016/j.tca.2006.11.021

in the spent fuel. There are several literatures on the oxidation of spent fuel [6,15–18]. However, the direct measurement of the oxidation rate of the spent fuel is very difficult in a laboratory because of dealing with high radioactive material. As a result, simulated spent fuel has usually been used to estimate the properties of an irradiated fuel such as the thermophysical properties, fission gas release and oxidation behavior [18–20]. Simulated spent fuel provides a convenient way to investigate the intrinsic fuel properties.

Thomas et al. [18] reported that air-oxidation of spent $UO_2$ fuel at temperatures near 473 K produced a persistent, cubic $U_4O_9$ without forming $U_3O_8$. $U_4O_9$ was converted to $U_3O_8$ above 523 K without producing intermediate phases such as $U_3O_7$. They also argued that the gadolinia forming the solid solution in the $UO_2$ matrix stabilized $U_4O_9$ and delayed $U_3O_8$ forming.

Choi et al. [19] studied the effects of the fission products on the rate of the $U_3O_8$ formation by oxidizing the simulated spent fuel in air at 523 K. They monitored the progress of oxidation by X-ray diffraction and found that the rate of the $U_3O_8$ formation declined with increasing burnup. Cobos et al. [20] studied oxidation behavior of simulated high burnup $UO_2$ fuel. During oxidation, the conversion of the simulated fuels to the (U, FP)$_4O_9$ and (U, FP)$_3O_8$-type phases was strongly delayed when the simulated burnup exceeded 80 GWd tM$^{-1}$.

In this paper oxidation behavior of the simulated spent fuel with dissolved fission products has been studied and presented using a TGA in the temperature range of 573–873 K in air in order to establish the oxidation temperature and time of the OREOX process during fabrication of DUPIC fuel. That of the $UO_2$ sintered pellet has also been measured for the purpose of comparison.

## 2. Experimental

### 2.1. Sample preparation and characterization

$UO_2$ and simulated spent fuel pellets with an equivalent burnup of 6 at.% were used in this study. The specimens were fabricated by compaction and sintering the powder prepared by adding stable oxides as surrogates for the fission products into $UO_2$. The fission product composition of the irradiated fuel was determined by its initial enrichment and irradiation history. The ORIGEN (Oak Ridge Isotope Generation and Depletion) code was used to calculate the compositions of the fission products which were added into the $UO_2$ powder. In this study, only the fission products forming solid solutions in the $UO_2$ matrix were added in order to confirm the effect of solid solutions on oxidation behavior of the simulated spent fuel. The contents of the fission products added into the $UO_2$ powder are shown in Table 1.

To prepare the simulated spent fuel, mixed powder of $UO_2$ and the additives were pressed with 300 MN m$^{-2}$ into green pellets, and sintered at 1973 K for 4 h in a flowing 100% $H_2$ gas stream. Complete descriptions of the fabrication methods and characterization results have been provided in the previous publication [21]. The theoretical density of the simulated spent fuel was calculated by assuming that the fission products added to the $UO_2$ were fully formed solid solutions with $UO_2$. The density and the grain size of the simulated spent fuel with the solid solutions used for the measurement were 10.49 g cm$^{-3}$ (96.9% of theoretical density) and 9.5 μm, respectively. It is also assumed that the specimens used in the experiment are stoichiometric, for they are sintered in conditions of 100% $H_2$ at a high temperature. The microstructures of the pellets are shown in Fig. 1. $UO_2$ and simulated fuel have almost the same microstructure and grain size. The densities of the $UO_2$ pellets for the density effect test were 10.37, 10.62 and 10.74 g cm$^{-3}$ (94.64, 96.88 and 97.96% of theoretical density). Disk samples having an average dimension of 8.5 mm in diameter and 1.4 mm in thickness were cut from the sintered pellets of the simulated fuel and $UO_2$ fuel. The initial average weight and surface area of a specimen was 0.8 g and 1.51 cm$^2$ abraded with 600 grit silicon-carbide paper, washed in acetone in an ultrasonic cleaner, and rinsed with ethyl alcohol.

Table 1
Contents of the surrogates for the fission products added to the $UO_2$ powder

| Fission products | Simulated spent fuel (wt.%) |
|---|---|
| Sr (SrO) | 0.173 |
| Y ($Y_2O_3$) | 0.144 |
| Zr ($ZrO_2$) | 0.723 |
| La ($La_2O_3$) | 0.245 |
| Ce ($CeO_2$) | 0.477 |
| Nd ($Nd_2O_3$) | 0.816 |
| Total | 2.578 |

### 2.2. Experimental procedure

The experiment was carried out in air (flow rate: 10 l h$^{-1}$. at an atmospheric pressure), and the furnace was rapidly heated up with constant heating rate (50 K min$^{-1}$) and maintained at a desired set temperature. To modify the buoyancy effect, a weight gain was ignored during the heating stage and was tared at an experimental temperature. It is reasonable to ignore the weight gain during the initial heat up time because the weight gains during the initial heat up time are 0.01, 0.3, 0.39 and 0.42% of the weight gain after a complete oxidation, at 573, 673, 773 and 873 K, respectively. Weight gain was measured continuously by the microbalance and stored in a personal computer.

## 3. Results and discussion

### 3.1. Oxidation reaction

It is well known that the oxidation of $UO_2$ is a two-step reaction:

$$UO_2 \rightarrow U_3O_7/U_4O_9 \rightarrow U_3O_8$$

Formation of $U_3O_7/U_4O_9$ from $UO_2$ involves a slight volume reduction. In contrast, $U_3O_8$ has a distinctly different crystal structure and a density that is 23% less than that of $UO_2$, which corresponds to the 36% volume increase. When $UO_2$ is oxidized

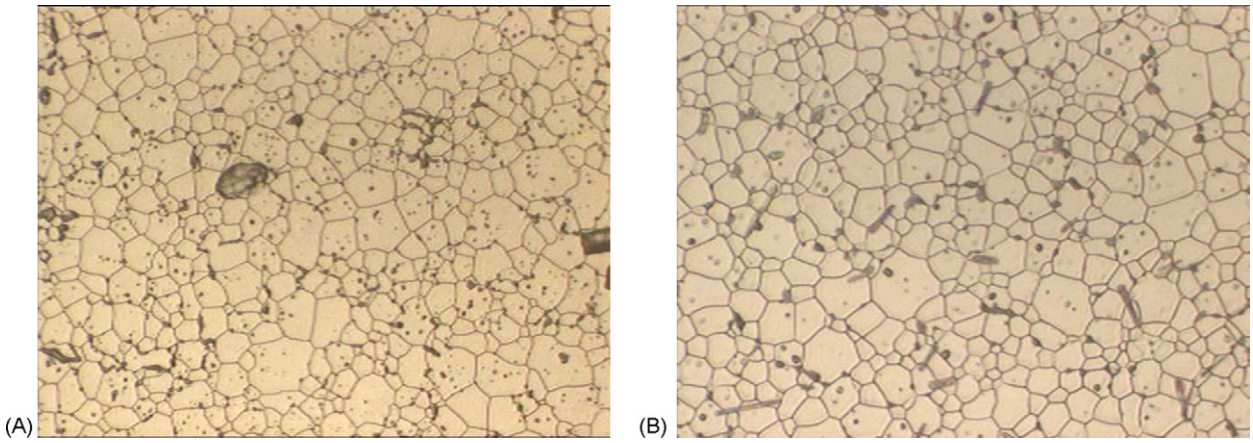


Fig. 1. Optical microscope images of $UO_2$ (A) and 6 at.% burnup simulated fuel with the dissolved fission products (B) (500×).

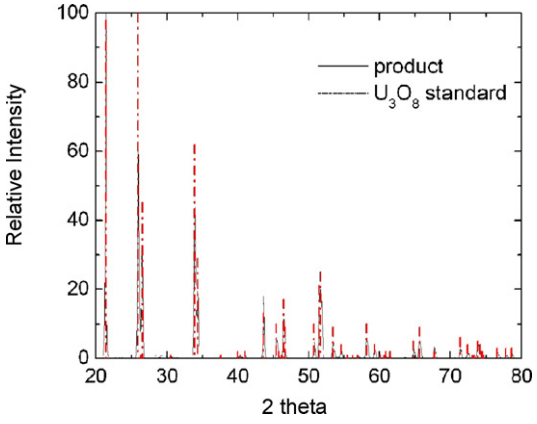


Fig. 2. XRD pattern of the products after the oxidation of simulated spent fuel.

in air, the specimen of the $UO_2$ pellet is fragmented and pulverized to powder due to the volume increase. In this study, the specimen of the simulated spent fuel pellet was pulverized to powder and it was transformed to $(U, FP)_3O_8$ after the full oxidation. The XRD pattern after complete oxidation is shown in Fig. 2. This result is in agreement with other results [18,20]. Thomas et al. [18] reported that air-oxidation of $UO_2$ spent fuel at temperatures near 473 K produced a persistent and cubic $U_4O_9$, and further oxidation of the $U_4O_9$ to $U_3O_8$ was detected in tests performed above 523 K without producing an intermediate phase such as $U_3O_7$. Cobos et al. [20] reported that in the low burnup range (<90 GWd $tM^{-1}$) one-step oxidation from $(U, FP)O_2$ to $(U, FP)_3O_8$ was observed, while in the high burnup range (>115 GWd $tM^{-1}$) a two-step oxidation curve ($(U, FP)O_2 \rightarrow (U, FP)_4O_9 \rightarrow (U, FP)_3O_8$) was observed.

### 3.2. Oxidation rates

The rate of the formation of $U_3O_8$ is generally modeled with a nucleation-and-growth expression [11]. Typical oxidation curves of the simulated spent fuel pellet with the fission products in solid solution with $UO_2$ are shown in Fig. 3. Results are shown as the fraction reacted ($\alpha$) versus time. The oxidation of simulated spent fuel proceeds slowly at the initial stage of reaction and increases more sharply after a certain time until decreasing due to slow reaction at the end of the experiment. The oxidation curves of simulated spent fuel display sigmoidal reaction kinetics which follows the nucleation-and-growth mechanism of the formation of $U_3O_8$. This profile is similar to those of other studies. You et al. [6] reporting on oxidation behavior of $UO_2$ in air stated that weight gain of non-irradiated $UO_2$ was characterized by the S-shape curve. As expected, oxidation rates of fuels increase with temperature. At 873 K, oxidation proceeds faster up to 60% oxidation, while after 60% oxidation the

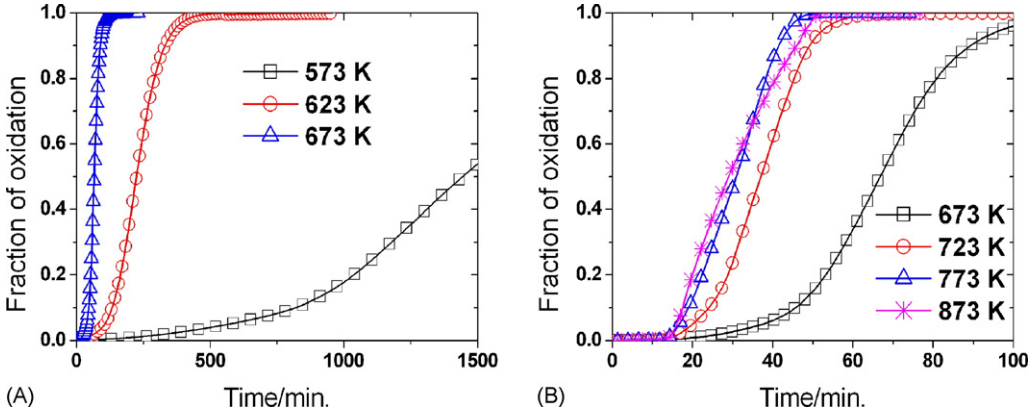


Fig. 3. Fraction reacted-time curve for oxidation of simulated spent fuel with the dissolved fission products at 573–873 K.

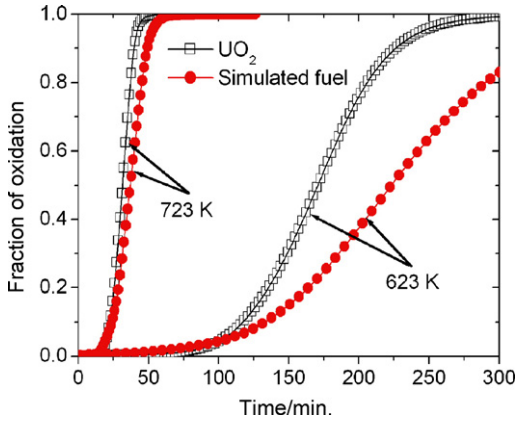


Fig. 4. Oxidation curves of simulated spent fuel and $UO_2$ at 623 and 732 K.

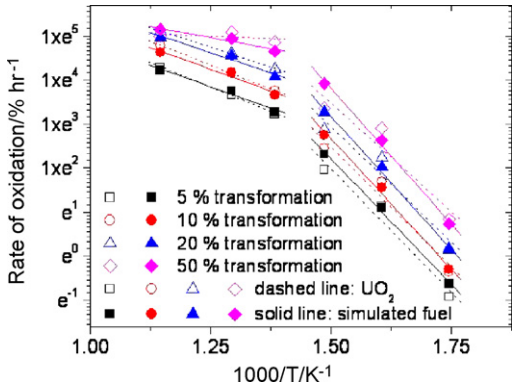


Fig. 5. Arrhenius plot for the oxidation of simulated spent fuel (solid symbols and lines) and $UO_2$ (dashed lines and hollow symbols) at 5 (squares), 10 (circles) 30 (triangle) and 50 (diamond)% transformation to $U_3O_8$.

process becomes slower than that at 723 K. This result agrees with the result of Peakall and Antill [22] who argued that this phenomenon appeared due to the increase in the thickness of products through which the oxygen had to be diffused as the particle size of the product was increased with the temperature. The mechanism of such thickening is probably associated with the increase in the plasticity of the products which allows the stresses in the film to be relieved by deformation rather than cracking.

The oxidation curves of the simulated spent fuel and $UO_2$ at 623 and 723 K are shown in Fig. 4 for the purpose of comparison between with and without solid solution in the $UO_2$ matrix. From the figure the oxidation of the simulated spent fuel proceeds slower than that of $UO_2$. This result fully agrees with the other results that gadolinia forming the solid solution in $UO_2$ matrix stabilized $U_4O_9$ and delayed $U_3O_8$ forming [18] and oxidation behavior of the simulated spent fuel shows a marked delay of transformations to the (U, FP)$_4O_9$ and (U, FP)$_3O_8$ phases [20].

To observe the reaction rate of the simulated spent fuel and $UO_2$ with variation of the temperature, the reaction rates at oxidations of 10%, 20% and 50% are shown in Table 2.

The reaction rates of the simulated spent fuel in the range of the experimental temperature except for 673 K are lower than those of $UO_2$. At 673 K, the reaction rate of the simulated spent fuel is higher than that of $UO_2$.

This is thought to be due to the different oxidation mechanisms of $UO_2$ and (U, FP)$O_2$ and more studies to understand this phenomena are necessary.

The fraction of the oxidation per unit time for 5, 10, 20 and 50% transformation versus the reciprocal of the temperature is displayed in Fig. 5. The oxidation fraction per unit time could be expressed by the Arrhenius type as follows:

$$k = k_0\, e^{-E_a/RT}$$

where $k$ (% h$^{-1}$) is the reaction fraction, $k_0$ (% h$^{-1}$) is the frequency factor, $E_a$ (kJ mol$^{-1}$) is the activation energy, $R$ (J mol$^{-1}$ K$^{-1}$)is the universe gas constant and $T$ (K) is the absolute temperature.

From the Arrhenius type of expression for the rate equation, activation energies and frequency factors of simulated spent fuel and $UO_2$ for 5, 10, 20 and 50% transformation were calculated. These results are shown in Fig. 6. There are transition points between 673 and 723 K and the activation energies in the low temperature range of 573–673 K are higher than those in the high temperature range of 573–673 K as You et al. [6] and Hasting et al. [16] suggested. The activation energies of simulated spent fuel are higher than those of $UO_2$. This result agrees with the other results that the activation energy of $UO_2$ doped with neodymium increases with the neodymium concentration [11]. For the simulated spent fuel, the activation energies in the range of 573–673 K are 94.61–102.56 kJ mol$^{-1}$ and they increase with the oxidation progress. This result is in good agreement with the other results. You et al. [6] estimated the activation energy for the oxidation of the spent LWR fuel in the range of 573 to 673 K to be 94.5 kJ mol$^{-1}$, which is slightly lower than that of our results for oxidation of the simulated fuel.

Table 2
Oxidation rates of simulated spent fuel and $UO_2$ at gains of 10%, 20% and 50%

| Temperature (K) | Rate of simulated fuel (% h$^{-1}$) | | | Rate of $UO_2$ (% h$^{-1}$) | | |
|---|---|---|---|---|---|---|
| | 10% | 20% | 50% | 10% | 20% | 50% |
| 573 | 0.6381 | 1.1629 | 2.0853 | 0.6990 | 1.2035 | 2.3202 |
| 623 | 4.7438 | 7.6186 | 13.843 | 5.4151 | 9.3023 | 18.259 |
| 673 | 15.756 | 26.310 | 50.641 | 11.429 | 17.699 | 28.874 |
| 723 | 38.986 | 59.435 | 105.67 | 42.553 | 70.175 | 130.43 |
| 773 | 64.171 | 94.414 | 140.78 | 64.516 | 100.84 | 163.04 |
| 873 | 102.21 | 144.40 | 172.71 | 120.00 | 166.67 | 148.51 |

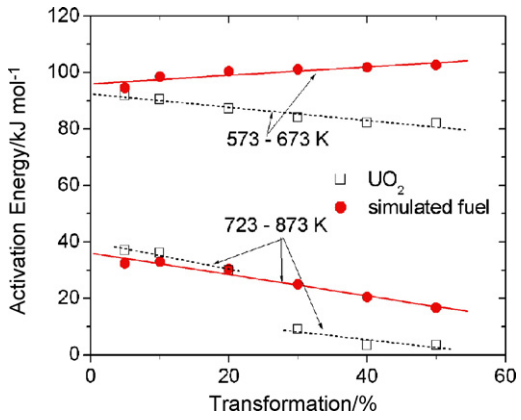


Fig. 6. Activation energies of simulated spent fuel and $UO_2$ vs. transformation to $U_3O_8$.

The results obtained in this study are useful to establish the oxidation temperature and time of the OREOX process during fabrication of the DUPIC fuel.

## 4. Conclusions

Analyses of the TGA and XRD patterns to observe the oxidation of the simulated spent fuel with dissolved the fission products have been carried out and the following conclusions could be made.

(1) From the XRD study, the simulated spent fuel with the dissolved fission products converted to $U_3O_8$, in the temperature range of 573–873 K.
(2) Oxidation curves of simulated spent fuel displayed sigmoidal reaction kinetics which follows the nucleation-and growth mechanism of the formation of $U_3O_8$.
(3) The fission products forming solid solution in the $UO_2$ matrix delayed $U_3O_8$ forming.
(4) The activation energies of the simulated spent fuel are higher than those of $UO_2$.
(5) There are transition points in the rate of the oxidation of simulated fuel and $UO_2$ between 673 and 723 K and the activation energies in the low temperature range of 573–673 K are higher than those in the high temperature range of 573–673 K.
(6) The data measured and calculated in this study will be useful for fabrication of the DUPIC fuel.

## Acknowledgement

This work was performed under the Long and Mid-Term Nuclear R&D program sponsored by the Ministry of Science and Technology.

## References

[1] I.J. Hastings, P.G. Boczar, C.J. Allan, M. Gacesa, Proceedings of the Sixth KAIF/KNS Annual Conference, Seoul, Korea, 1991.
[2] M.S. Yang, et al., Proceedings of the International Conference on Future Nuclear Systems: Emerging Fuel Cycles and Waste Disposal Options Global '93, Seattle, Washington, 1993.
[3] P. Tayler, D.D. Wood, A.M. Duclos Mate, J. Nucl. Mater. 189 (1992) 116.
[4] S.R. Teixeira, K. Imakura, J. Nucl. Mater. 178 (1991) 33.
[5] L.E. Thomas, O.D. Slagle, R.E. Einziger, J. Nucl. Mater. 184 (1991) 117.
[6] G.S. You, K.S. Kim, Ro.F S.G., E.K. Kim, J. Korean Nucl. Soc. 27 (1995) 67.
[7] P.G. Lucuta, Hj. Matzke, R.A. Verrall, J. Nucl. Mater. 223 (1995) 51.
[8] L.A. Goldsmith, J.A.M. Douglas, UKAEA Report TGR-2103, 1971.
[9] R.C. Hawkings, A.S. Bain, AECL Report AECL-1790, 1963.
[10] D.R. Olander, TID-26711-P1, 1976.
[11] R.J. McEachern, P. Taylor, J. Nucl. Mater. 254 (1998) 87.
[12] T.R. Griffiths, V.A. Volkovich, J. Nucl. Mater. 274 (1999) 229.
[13] D. Majumda, et al., DOE/ID-10423, 1992.
[14] K.K. Bae, B.G. Kim, Y.W. Lee, M.S. Yang, H.S. Park, J. Nucl. Mater. 209 (1994) 274.
[15] J. Novak, I.J. Hastings, E. Mizzan, R.J. Chenier, Nucl. Tech. 63 (1983) 254.
[16] J. Hasting, D.H. Rose, J.R. Kelm, D.A. Irvine, J. Novak, J. Am. Ceram. Soc. 69 (2) (1986) C–16.
[17] K.M. Wasywich, W.H. Hocking, D.W. Shoesmith, P. Taylor, Nucl. Tech. 104 (1993) 309.
[18] L.E. Thomas, R.E. Einziger, H.C. Buchanan, J. Nucl. Mater. 201 (1993) 310.
[19] J.W. Choi, R.J. McEachern, P. Taylor, D.D. Wood, J. Nucl. Mater. 230 (1996) 250.
[20] J. Cobos, D. Papaioannou, J. Spino, M. Coquerelle, J. Alloys Comp. Mater. 271–273 (1994) 601.
[21] K.H. Kang, K.C. Song, J.S. Moon, H.S. Park, M.S. Yang, Metals Mater. 6 (2000) 583.
[22] S. Aronson, R.B. Roof, J.R. and, J. Belle, J. Chem. Phys. 27 (1957) 137.